EFFECT OF DYNAMIC TURBULENCE OF THE ATMOSPHERIC BOUNDARY LAYER ON THE ACCURACY OF DOPPLER–LIDAR WIND–VELOCITY MEASUREMENTS

V.A. Banakh, Ch. Werner, F. Köpp, and I.N. Smalikho

Institute of Atmospheric Optics,
Siberian Branch of the Russian Academy of Sciences, Tomsk
Institute of Optoelectronics DLR,
Oberpfaffenhofen, D–82230 Wessling, Germany
Received July 27, 1993

In this paper we present a theoretical analysis of the relative error ε_{xy} in measurements of the mean wind velocity with a cw Doppler scanning lidar. Our analysis takes into account spatial and temporal averaging of the wind velocity fluctuations and the dependence of this error on the turbulent state of the atmospheric boundary layer during the measurements. Our theoretical results have been verified in the experiments with a Doppler lidar at the Institute of Optoelectronics. The experimental data have shown satisfactory agreement with the theoretical results. It is shown that under conditions of stable atmospheric stratification and at altitudes $h > 150-200$ m the measurements of mean wind velocity become representative ($\varepsilon_{xy} \leq 10\%$) already after one scan. In the ground atmospheric layer ($h = 60$ m) under conditions of neutral stratification the error $\varepsilon_{xy} < 10-12\%$ can be obtained only after five scans ($N = 5$).

INTRODUCTION

The turbulence is one of the main sources of errors in mean wind velocity measurements in the atmospheric boundary layer with the use of a Doppler lidar. As is known, in the atmosphere, especially in its lower layers, the velocity of air flow changes randomly in space and time. The difference between the wind velocity averaged over the entire air flow and velocity being measured over finite period in the bounded sensed volume in lidar sensing may be interpreted as a random error in the mean wind velocity measurements. The representativity of the lidar measurements of the mean wind velocity can be judged from the magnitude of this error.

Varying the sensing volume dimensions and measurement time, we can obtain the acceptable values of the random errors due to averaging. Hence the representativity of lidar measurements of mean wind velocity depends on the procedure of temporal and spatial averaging of scattered lidar signal. In addition we must bear in mind that measurement accuracy providing the representativity of measurements depends on both characteristic dimensions of turbulent eddies and strength of turbulent mixing. In their turn they are determined by the outer dynamic and thermal parameters of the atmospheric boundary layer such as the roughness parameter, the vertical turbulent heat flux, and so on.

This paper presents the results of theoretical and experimental investigation of the representativity of mean wind velocity measurements made by means of a coherent cw Doppler lidar, which uses the conical scan technique,[1] in the boundary layer of the atmosphere under different turbulent conditions.

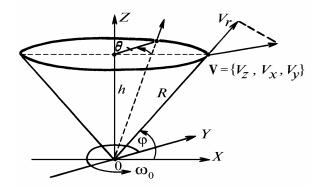## CALCULATION OF MEASUREMENT ERROR

FIG. 1. Schematic illustration of the geometry of the conically scanning lidar.

The technique of conical scan of the laser beam around the vertical axis z (see Fig. 1) makes it possible to determine the components of the wind velocity vector. Really in the case of a homogeneous flow the value of V_D measured through Doppler frequency shift f_D of the received lidar signal

$$V_D = (\lambda/2)\, f_D \qquad (1)$$

coincides with the radial component V_r of the velocity vector $\mathbf{V}(V_D = V_r)$. The radial component V_r is related to the components V_z, V_x, and V_y of the vector $\mathbf{V}$ by the formula

© 1993 Institute of Atmospheric Optics

$$V_r = V_z \sin \varphi + V_x \cos \varphi \cos \theta + V_y \cos \varphi \sin \theta , \qquad (2)$$

where θ is the azimuth angle, φ is the elevation angle of scan cone generatrix with respect to the horizon. When the components V_z, V_x, and V_y of the velocity vector $\mathbf{V}$ are constant, the dependence of V_r and consequently V_D on the angle θ is sinusoidal, and these components may be easy determined from this sinusoidal dependence.[1]

In the real atmosphere the wind velocity $\mathbf{V}$ is a random function of coordinates $\mathbf{r} = \{x, y, z\}$ and time t because of turbulence. In this situation information about the components of the wind velocity vector can be obtained by fitting the measured dependence of V_D on θ into the sinusoidal model by the least-squares method[1–4]

$$V_{Lz} = \frac{1}{\sin \varphi} \frac{1}{T} \int_0^T dt\, V_D(t), \quad V_{Lx} = \frac{1}{\cos \varphi} \frac{2}{T} \int_0^T dt\, V_D(t) \cos \omega_0 t ,$$

$$V_{Ly} = \frac{1}{\cos \varphi} \frac{2}{T} \int_0^T dt\, V_D(t) \sin \omega_0 t , \qquad (3)$$

where V_{Lz}, V_{Lx}, and V_{Ly} are the estimates of the wind velocity components obtained from lidar measurements, $T = 2\pi N/\omega_0$ is the measurement time, N is the number of revolutions, and ω_0 is the angular velocity of laser beam rotation around the vertical axis.

As noted above, the velocity $V_D(t)$ is determined through the Doppler frequency f_D corresponding to the frequency of centroid of the lidar signal power spectrum. This frequency depends on the characteristics of the medium, viewing geometry, parameters of the receiving–transmitting system, and statistics of the measurable wind velocity[5]

$$\hat{f}_D(t) = \frac{2}{\lambda} \int_0^\infty dz'\, V_r(z', 0, t)\, Q_s(z', t) , \qquad (4)$$

where

$$Q_s(z', t) = \frac{\dfrac{\sigma_t B_\pi \rho_c(z', t)}{g^2(z')} \exp\left[-2 \displaystyle\int_0^{z'} dz''\, \sigma_t \rho_c(z'', t) \right]}{\displaystyle\int_0^\infty dz'\, \frac{\sigma_t B_\pi \rho_c(z', t)}{g^2(z')} \exp\left[-2 \displaystyle\int_0^{z'} dz''\, \sigma_t \rho_c(z'', t) \right]} \qquad (5)$$

is the function characterizing the geometry of sensing volume and its scattering property, σ_t is the total scattering cross section, B_π is the scattering phase function, ρ_c is the concentration of scattering particles, a_0 is the beam radius in the initial plane $z'=0$, $a_0 g(z') = a_0 \left[\left(1 - \dfrac{z'}{R} \right)^2 + \dfrac{z'^2}{(k a_0^2)^2} \right]^{1/2}$ is the diffraction beam radius, R is the curvature radius of initial phase front of the beam, and $k = 2\pi/\lambda$ is the wave number.

The maximum contribution to the Doppler frequency shift comes from particles moving with the velocities $V_r(z')$ in the vicinity of the point $z' = z_m$, at which the function $Q_s(z')$ reaches its maximum. Thus the effective length Δz of the sensed volume may be determined as

$$\Delta z = \int_0^\infty dz'\, Q_s(z') / Q_s(z_m) .$$

The atmospheric turbulence will be considered stationary and horizontally homogeneous and the mean wind velocity vector at the altitude h will be directed along the x axis of the Cartesian coordinate system

$$<\mathbf{V}> = \{0, U(h), 0\} , \qquad (6)$$

where U is the mean wind velocity. In accordance with Eqs. (1), (3), and (4) we have

$$<V_{Lz}> \approx <V_{Ly}> \approx 0 , \quad <V_{Lx}> \approx U(h) . \qquad (7)$$

The relative error in lidar measurements of the mean wind velocity may be determined as

$$\varepsilon_{xy} = \sqrt{< (V_{xy} - U)^2>} / U , \qquad (8)$$

where $V_{xy} = \sqrt{V_{Lx}^2 + V_{Ly}^2}$ is the measured value of the horizontal wind velocity component. Assuming that $|V_{Lx} - U|$, $|V_{Ly}| \ll U$, from Eqs. (1), (3), (4), and (8) we derive the formula

$$\varepsilon_{xy} = \frac{2}{\cos \varphi\, U T} \sqrt{\int_0^T \int dt'\, dt''\, F(t', t'') \cos \omega_0 t' \cos \omega_0 t''}, \qquad (9)$$

where

$$F(t', t'') = \int_0^\infty \int dz'\, dz''\, Q_s(z')\, Q_s(z'')\, K_r(z', z'', t', t'') ,$$

$$K_r(z', z'', t', t'') =$$
$$= <[V_r(\mathbf{r}(z', t'), t') - <V_r(\mathbf{r}(z', t'), t')>] \times$$

$$\times [V_r(\mathbf{r}(z'', t''), t'') - <V_r(\mathbf{r}(z'', t''), t'') >] > \qquad (10)$$

is the spatiotemporal correlation function for the radial wind velocity component and $\mathbf{r}(z', t') = \{z'\sin\varphi,\ z'\cos\varphi \cos\omega_0 t',\ z'\cos\varphi \sin\omega_0 t'\}$. The use of Taylor's hypothesis of "frozen" turbulence[6,7] and substitution of relations (3) into Eq. (10) yields

$$K_r(z', z'', t', t'') = \cos^2 \varphi\, [K_{xx}(\mathbf{p}) \cos \omega_0 t' \cos \omega_0 t'' +$$

$$+ K_{yy}(\mathbf{p}) \sin \omega_0 t' \sin \omega_0 t'' + K_{xy}(\mathbf{p}) (\cos \omega_0 t' \sin \omega_0 t'' +$$

$$+ \sin \omega_0 t' \cos \omega_0 t'')] + \sin \varphi \cos \varphi\, [K_{xz}(\mathbf{p}) (\cos \omega_0 t' + \cos \omega_0 t'') +$$

$$+ K_{yz}(\mathbf{p}) (\sin \omega_0 t' + \sin \omega_0 t'')] + \sin^2 \varphi\, K_{zz}(\mathbf{p}) , \qquad (11)$$

where $\mathbf{p} = \mathbf{r}(z', t') - \mathbf{r}(z'', t'') + <\mathbf{V}>(t' - t'')$,

$$K_{lk}(\mathbf{p}) = <[V_l(\mathbf{r} + \mathbf{p}, 0) - <V_l>] [V_k(\mathbf{r}, 0) - <V_k>] > \qquad (12)$$

is the spatial correlation tensor of the wind velocity fluctuations, and $l, k = z, x, y$.

For simplicity we further assume that the anisotropy of wind fluctuations insignificantly affects the error ε_{xy} (see Ref. 7). In this instance the correlation tensor is expressed as follows:

$$K_{l\,k}(\mathbf{p}) = K_u(p)\,\delta_{l\,k} + \frac{1}{2}\,p\,\frac{d\,K_u(p)}{d\,p}\left[d_{l\,k} - \frac{p_l\,p_k}{p^2}\right], \qquad (13)$$

were $K_u(p)$ denotes the function of the longitudinal spatial correlation of wind velocity, $\delta_{ll} = 1$, $\delta_{l \neq k} = 0$, and $p = |\mathbf{p}|$.

Thus in order to calculate the measurement error ε_{xy} it is necessary to know the function $K_u(p)$. Among the known models for this function the exponential model

$$K_u(p) = \sigma_u^2 \exp(-p/l_u), \qquad (14)$$

is most widely used, where σ_u^2 is the fluctuation variance and $l_u = \int\limits_0^\infty dp\,K_u(p)/\sigma_u^2$ is the integral correlation length for the longitudinal component of the wind velocity. The use of the von Karman model of the spatial spectrum of turbulence

$$S_u(\eta) = 0.637\,\sigma_u^2\,l_u\,/\,(1 + 1.8\,l_u^2\,\eta^2)^{5/6} \qquad (15)$$

allows us to obtain the relation of the parameters σ_u^2 and l_u of the function $K_u(\mathbf{p})$ with the turbulent energy dissipation rate ε_T. Really for high–frequency range $(\eta \gg 1/l_u)$ Eq. (15) yields

$$S_u(\eta) = 0.394\,\sigma_u^2\,l_u^{-2/3}\,\eta^{-5/3}. \qquad (16)$$

For the inertial interval the turbulence spectrum is written as[6,7]

$$S_u(\eta) = C_k\,\varepsilon_T^{2/3}\,\eta^{-5/3}, \qquad (17)$$

where C_k is the Kolmogorov constant, which takes the values in the range between 0.33 and 0.5 according to Ref. 7. From Eqs. (16) and (17) it follows that

$$l_u = \left(\frac{0.394}{C_k}\right)^{3/2}\frac{\sigma_u^3}{\varepsilon_T}. \qquad (18)$$

In the atmospheric boundary layer the parameters U, σ_u^2, l_u, and ε_T depend primarily on two dynamical parameters, namely, the geostrophic wind velocity $G = |\Delta P|/(f\rho_0)$ (where ΔP is the horizontal pressure gradient, ρ_0 is the air density, and f is the Coriolis parameter) and the roughness parameter z_0, and one thermal parameter, namely the vertical turbulent heat flux $H = C_p\,\rho_0\,K_T(\gamma - \gamma_a)$, where C_p is the air heat capacity, K_T is the turbulent exchange coefficient, $\gamma = -dT_0/dz$ is the lapse rate of the mean temperature T_0, and γ_a is the adiabatic lapse rate.[6,7,8,9] In the surface layer ($h < 20$–100 m) the turbulent heat flux H remains constant, and above this layer H depends on the altitude h because of diurnal variation of radiation regime of heating of the Earth surface and air.[9] The parameter, which is usually used for the description of thermal stratification, is the Monin–Obukhov length[7]

$$L = -u_*^3\,/\,(g_0\,\kappa\,H\,/\,T_0\,\rho_0\,C_p), \qquad (19)$$

where $\kappa \sim 0.4$ is the von Karman constant, g_0 is the acceleration due to gravity, and, u_* is the friction velocity.

The equation for the mean velocity in the atmospheric surface layer has the following form[7]:

$$\frac{d\,U(z)}{d\,z} = \frac{u_*\,\varphi_u(z)}{k\,z}, \qquad (20)$$

where φ_u is some universal function of the dimensionless parameter $\zeta = z/L$. For neutral stratification $(\gamma = \gamma_a$, $H = 0$, $L = \infty)$ the function $\varphi_u(0) = 1$.

In order to find $U(z)$ let us use the empirical formula

$$\varphi_u(\zeta) = \begin{cases} 1 + 5\zeta, & \zeta \geq 0, \\ (1 - 15\zeta)^{-1/3}, & \zeta \leq 0, \end{cases} \qquad (21)$$

which is in satisfactory agreement with the experimental data of Ref. 10. Then, taking into account the condition $z_0 \ll |L|$, we can derive from Eq. (20) the approximate formula for the mean wind velocity in the form

$$U(z) = \frac{u_*}{k}\begin{cases} \ln\left(\dfrac{z}{z_0}\right) + 5\zeta, & \zeta \geq -\dfrac{1}{15}, \\[2mm] \ln\left(\dfrac{z}{z_0}\dfrac{1}{15|\zeta|}\right) - \dfrac{1}{3} + 3\,[1 - (15|\zeta|)^{-1/3}], & \zeta \leq -\dfrac{1}{15}. \end{cases} \qquad (22)$$

For calculations of ε_T and σ_u^2 we can use the formulas[7,11]

$$\varepsilon_T = \frac{u_*^3}{k\,z}\,[\varphi_u(\zeta) - \zeta], \qquad (23)$$

$$\sigma_u^2 = u_*^2\left[C_v^2\sqrt{1 - \zeta\,/\,\varphi_u(\zeta)} + \frac{C_u^2 - C_v^2}{\sqrt{1 - \zeta\,/\,\varphi_u(\zeta)}}\right], \qquad (24)$$

where C_v and C_u are empirical constants ($C_v = 1.3 - 2.2$ and $C_u = 2.1 - 2.9$, see Ref. 6). The friction velocity u_* depends on the geostrophic wind velocity, the roughness parameter, the Coriolis parameter, and the thermal stratification (stability). It can be calculated theoretically (see, for example, Refs. 7, 9, and 12), if information on the above–listed parameters G, z_0, f, and H is available, or be measured directly near the Earth surface using the known measurement procedure.[9] The correlation length l_u can be calculated by formulas (18), (21), (23), and (24).

The models (21)–(24) allow us to calculate u, σ_u^2, l_u, and ε_T at arbitrary altitude in the surface layer of stationary and horizontally homogeneous atmosphere, if the parameters z_0, L, and u_* are known. In general the theoretical models of these turbulent characteristics of the boundary layer can be created on the basis of numerical solution of corresponding equations (see, for example, Refs. 7, 9, 13, and 14). But in the case of neutral thermal stratification the simple empirical formulas[9,12–15]

$$\sigma_u(z) = \sigma_{uS}\exp(-C_1\,z/h_b), \qquad (25)$$

$$l_u(z) = \frac{l_{uS}(z)}{1 + C_2\dfrac{l_{uS}(z)}{h_b}}. \qquad (26)$$

can be used. Here σ_{uS}^2 and l_{uS} are the variance and the correlation length of the longitudinal wind velocity component, calculated by formulas for the surface layer (Eqs. (18), (23), and (24) for $\zeta = 0$), $h_B \approx \kappa u_* / |f|$ is the effective atmospheric boundary layer thickness ($h_B \sim 1$ km, see Ref. 7), C_1 and C_2 are empirical constants, which are equal to 0.8 and 2.5 according to the data of experimental studies performed in Ref. 15.

From Eq. (9) it follows that when V_{xy} is measured, temporal as well as horizontal (over the base of a scan cone) and longitudinal (over the beam axis) spatial averagings of the wind velocity fluctuations take place simultaneously. The parameters of the spatial averaging are R and φ, and the parameters of the temporal averaging are N and ω_0. We must answer the question: What values of these parameters provide for the representative measurements of the mean wind velocity? In order to answer this question, we must estimate the measurement error ε_{xy}. According to Eqs. (9)–(15), the error ε_{xy} depends strongly on the atmospheric parameters σ_u^2, l_u, and U, and the expression for ε_{xy} can be represented by the product of the ratio σ_u^2/U, describing the turbulence strength, and the function of the parameters a/l_u ($a = R \cos\varphi$ is the radius of the base of a scan cone), $\Delta z/l_u$, $U/(l_u \omega_0)$, and N. It is obvious that the larger are the ratios a/l_u and $\Delta z/l_u$, the greater is the efficiency of spatial averaging, and the larger is the ratio $U/(l_u \omega_0)$, the greater is the efficiency of temporal averaging. We note that usually $\varepsilon_{xy} \leq 10\%$ is sufficient for representativity of mean wind velocity measurements.

Figures 2 and 3 show the theoretical estimates of the error ε_{xy} in the wind velocity measurements performed with a Doppler lidar in the atmospheric surface layer at the altitude $h = 60$ m. The calculations were performed at $\lambda = 10.6$ μm for $a_0 = 15$ cm, $t_r = 2\pi/\omega_0 = 12$ s, $U = 10$ m/s, and $\sigma_u/U = 0.15$.

Figure 2 illustrates the dependence of ε_{xy} on the number of revolutions N at the elevation angle $\varphi = 45°$ (see Fig. 1) for different values of the correlation length $l_u = 300(1)$, $200(2)$, and 100 m (3). Solid lines show the results of calculations based on Eq. (9), dashed lines show the results of calculations by the formula

$$\varepsilon_{xy} = \frac{\sigma_u}{U} \sqrt{\frac{l_u \omega_0}{\pi U N}} \, , \qquad (27)$$

which was obtained by Kristensen et al.[16] under condition $N \gg l_u/(U t_r)$. It is seen from Fig. 2 that formula (27) gives the results which are close to that calculated by Eq. (9) only when $N > 10$. According to curve 2 for $l_u = 200$ m (the length, which is realized under condition of neutral stratification) the lidar measurements become representative (the error $\varepsilon_{xy} \leq 10\%$) beginning with $N \approx 5$, if we use Eq. (9), and with $N \approx 8$, if asymptotical formula (27) is used for estimation.

Different values of the length l_u may be thought of as corresponding to different types of thermal stratification. Thus depending on the class of atmospheric stability (values of l_u), the representativity of lidar wind velocity measurements is achieved for different numbers of

revolutions: $N \geq 2$ for $l_u = 100$ m, $N \geq 5$ for $l_u = 200$ m, and $N \geq 8$ for $l_u = 300$ m.
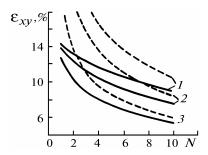

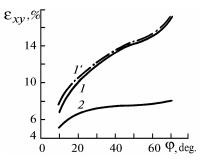FIG. 2. Measurement error ε_{xy} versus the number of revolutions N.

FIG. 3. Measurement error ε_{xy} versus the elevation angle φ for $N = 1$ (1 and 1') and 10(2).

Figure 3 shows ε_{xy} dependence on the elevation angle φ calculated at the fixed altitude h. Since in this case the radius of the base of a scan cone a and the length of a sounded volume along the beam axis Δz vary with the angle φ, the results shown in this figure serve as a good example of the spatial averaging effect on the error in Doppler-lidar measurements of mean wind velocity. Increase of the angle φ causes the decrease of the averaged volume and therefore, increase of ε_{xy}. In particular, at $\varphi = 60°$ and $N = 1$ (curve 1) the relative error in lidar measurements becomes larger than the relative variance of the wind velocity fluctuations σ_u/U ($\varepsilon_{xy} > \sigma_u/U = 0.15$). In the limiting case $\varphi \to 90°$ the value of $\varepsilon_{xy} \sim \tan\varphi$. When $\varphi \to 0°$, the averaged volume increases and $\varepsilon_{xy} \to 0$.

Dot-dashed curve 1 in Fig. 3 shows the result of calculation of ε_{xy} without regard for the spatial averaging along a laser beam ($\Delta z = 0$). It is seen that in the region $\varphi \geq 10°$ the longitudinal averaging makes insignificant contribution as compared with the horizontal averaged over the cone circular base. The reason is that in the surface layer ($h < 100$ m) the radius of the base of a scan cone $a = h/\mathrm{tg}\varphi$ far exceeds the extension of a sounded volume along the beam axis $\Delta z = 0.5\,\lambda(h/a_0)^2/\sin^2\varphi$, that is, $a \gg \Delta z$. It seems likely that the effect of spatial longitudinal averaging on the value of ε_{xy} becomes pronounced only for high-altitude measurements in the atmospheric boundary layer, when the inverse inequality $a \leq \Delta z$ is fulfilled.
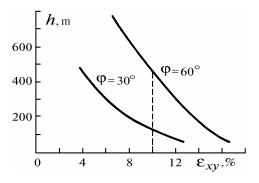
FIG. 4. Vertical profile of the measurement error ε_{xy}.

The curves in Fig. 4 illustrate the ε_{xy} dependence on the measurement altitude h for one revolution ($N = 1$) at two different elevation angles ($\varphi = 30$ and $60°$). In calculations, the models (18)–26) were used under conditions of neutral stratification and the friction velocity and roughness parameter were set $u_* = 0.65$ m/s and $z_0 = 0.24$ m. It can be seen that the error ε_{xy} decreases with the altitude increase and beginning with $h \gtrsim 150$ m it becomes less than 10% at $\varphi = 30°$. Thus already one revolution provides for the representativity of lidar measurement of the mean wind velocity at given conditions in the boundary layer. Because of greater degree of spatial averaging the error value decreases more rapidly at $\varphi = 30°$ than at $\varphi = 60°$.

EXPERIMENT

The measurements were carried out in the spring-summer season of 1992 in the south of Germany in Lichtenau. A Doppler lidar was located on the even ground, approximately 100×200 m in size, surrounded by trees and a few buildings. The ground was covered by grass about 20 cm high. The lidar sounding was accompanied by simultaneous measurements of the wind velocity with a cup anemometer located at an altitude of 60 m. The distance between the lidar and mast with the cup anemometer was about 50 m. Near the measurement site the roughness parameter z_0 was approximately equal to 0.24 m. Figure 5 shows the setup and geometry of the experiment.
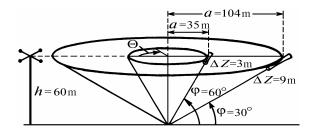

FIG. 5. Experimental geometry.

The class of thermal stratification was identified from the wind velocity and temperature measurements performed with the use of cup anemometers and thermometers placed at fixed altitudes h_i ($h_1 = 0.3$ m, $h_2 = 0.7$ m, $h_3 = 1.5$ m, $h_4 = 3$ m, and $h_5 = 6$ m). The data of cup-anemometer measurements were also used for estimation of the friction velocity u_* and the level of turbulent fluctuations of the wind velocity σ_u/U. To evaluate the effect of spatial averaging on the error ε_{xy}, the lidar measurements were carried out at two elevation angles

$\varphi = 30$ and $60°$. In this case the sensing range was adjusted in such a way as to measure at the same altitudes at both angles. The angular velocity was 30 deg/s for all measurements.

The measured wind velocities V_{xy} (in m/s) are shown in Figs. 6a–f. Points indicate the lidar data obtained for one revolution ($N = 1$), crosses and triangles denote the cup anemometer data averaged over periods of 2 and 10 min, respectively. Each run of lidar measurements shown in Figs. 6a–f consisted of ten independent measurements which were carried out at random intervals 2–10 min. In its turn each of these ten independent measurements was performed during the course of nine continuous revolutions of laser beam around the vertical axis.

The data were obtained under neutral (Fig. 6a, b, and d), stable (Fig. 6c), slightly unstable (Fig. 6e), and unstable (Fig. 6f) stratifications. In all the measurements the elevation angle φ was 30°, except for the data shown in Fig. 6b and obtained at $\varphi = 60°$. The data shown in Figs. 6a and b were obtained under identical turbulent conditions of the atmospheric surface layer. This allows us to estimate correctly the effect of spatial averaging on the lidar wind velocity measurement accuracy. It is clear that the points in Fig. 6a ($\varphi = 30°$) are less scattered than the lidar data in Fig. 6b ($\varphi = 60°$) because of greater degree of spatial averaging. The wide spread of the points in Fig. 6d is primarily connected with mesoscale variations of the wind velocity (apparently, gravitational waves with a period of ~20 min) rather than with atmospheric turbulence. Figures 6c and f illustrate the effect of atmospheric stability on the lidar wind velocity measurements for $N = 1$.

The code, used for processing of lidar data, allowed us to obtain the three components V_{Lz}, V_{Lx}, and V_{Ly} of the wind velocity vector for one revolution ($N = 1$). In order to estimate the horizontal wind velocity component V_{xy} for different numbers of revolutions N, we must use the formula

$$V_{xy}^j(N) = \frac{1}{N}\sqrt{\left[\sum_{k=1}^{N} V_{Lx}^j(k)\right]^2 + \left[\sum_{k=1}^{N} V_{Ly}^j(k)\right]^2}, \qquad (28)$$

where the independent measurements performed with the Doppler lidar are labelled by an index $j = 1, 2, ..., n$ ($n = 10$) and $N = 1, 2, ..., 9$. In Eq. (28) only the adjacent terms of the data series $V_{Lx}^j(k)$ and $V_{Ly}^j(k)$ of j–th measurement step are summed up so that summation in Eq. (28) is equivalent to integration in Eq. (3).

The errors in lidar measurements of mean wind velocity were calculated from the experimental data by the formula

$$\varepsilon_{xy}(N) = \sqrt{\frac{1}{n-1}\sum_{j=1}^{n}\left[\frac{V_{xy}^j(N)}{<V^j>} - 1\right]^2}, \qquad (29)$$

where $<V^j>$ is the estimate of the mean wind velocity. Assuming that the atmosphere was stationary in the course of measurements the results of which are shown in Figs. 6a, b, e, and f, the mean wind velocity was calculated by the formula

$$<V^j> = <V> = \frac{1}{n}\sum_{j=1}^{N} V_{xy}^j \quad (9).$$ In calculations of the measurement errors for the data shown in Figs. 6c and d, the cup anemometer data, averaged over the period $[t_j - (1/2)\Delta t, t_j + (1/2)\Delta t]$ at $\Delta t = 10$ min, were used for $<V^j>$ there by providing for mesoscale variations of wind velocity. It is obvious that the less is N, the larger number of ε_{xy} can be calculated from the data of the jth measurement due to different combinations of $V_{xy}^j(N)$. Thus for $N = 1$ we

can form 9 combinations of $V^j_{xy}(1)$ from the data series $\{V^j_{Lx}(1), ..., V^j_{Lx}(9)\}$, $\{V^j_{Ly}(1), ..., V^j_{Ly}(9)\}$ of the j–th measurement. For $N = 2$, there are 8 combinations of pairs $V^j_{xy}(2)$, consisting of neighboring values of the wind velocity, for $N = 3$ we have 7 combinations of three neighbouring values $V^j_{xy}(3)$, and so on. For $N = 9$ only one combination can be formed. The data on ε_{xy} corresponding to the given value of N are presented below as results of averaging over all the combinations available for the given N.

A comparison of the experimental values of the error ε_{xy} (in per cent) in the surface atmospheric layer with the theoretical results is shown in Fig. 7. Curves denote the results of theoretical calculations of ε_{xy} by formula (9). Symbols denote the errors calculated from the experimental data shown in Figs. 6a–f. It is seen that the theoretical and experimental data are in satisfactory agreement. This allows us to explain the behavior of the relative error ε_{xy} as a function of the number of revolutions N for different classes of atmospheric stability. As atmospheric stability increases ($h/L > 0$), the turbulence strength σ_u/U and the correlation length l_u decrease, and therefore, the accuracy of lidar measurements of the wind velocity improves. As Fig. 7 shows (points and solid line), in the case of stable stratification one revolution ($N = 1$) provides for the mean wind velocity measurements with the error $\varepsilon_{xy} < 10\%$. The accuracy of wind velocity measurements with the use of the Doppler lidar deteriorates with the increase of the atmospheric instability ($h/L < 0$) due to the increase in the parameters σ_u/U and l_u. As can be seen from Fig. 7, five revolutions ($N \approx 5$) provide for the mean wind velocity measurements with the error $\varepsilon_{xy} \lesssim 10$–12% in the case of neutral and slightly unstable stratifications at $\varphi = 30°$.

In order to check the theoretical conclusions about the behavior of ε_{xy} as a function of the altitude h, ten independent measurements of the wind velocity were carried out at altitudes of 60 m, 160 m, 260 m, and 360 m for $N = 1$ at $\varphi = 30°$. All measurements were performed for 40 minutes. Figure 8 shows the lidar data (points) and the wind velocity profile averaged over these data (dashed line).

Figure 9 illustrates the dependence of ε_{xy} on the altitude h. Solid line shows the result of calculation by formulas (9)–(14), (25), and (26). Points denote the results obtained from the experimental data shown in Fig. 8. Figure 9 confirms the theoretical conclusions (see Fig. 4) that the error ε_{xy} decreases rapidly as the measurement altitude h increases. Such behavior of ε_{xy} is explained by two reasons. On the one hand, the turbulence strength σ_u/U decreases as h increases, because the mean wind velocity increases with altitude, as can be seen from the preceding figure, and conversely, σ_u decreases, as it follows from formula (25). On the other hand, the spatial averaging becomes more efficient, since the ratios a/l_u and $\Delta z/l_u$ increase with altitude.

Really, according to Eq. (26) the parameter l_u at first increases with altitude h nonlinearly, and then saturates at the level h_B/C_2, when $h \to \infty$. At the same time, $a \sim h$ and $\Delta z \sim h^2$. This is illustrated by the following example. Let the parameters l_{uS}, h_B, and C_2 in Eq. (26) be $l_{uS}(z) = 5z$, $h_B = 1000$ m, and $C_2 = 2.5$. Then at $\varphi = 30°$ and altitude $h = 60$ m, we obtain $a \sim 104$ m, $\Delta z \sim 14$ m, and $l_u \sim 172$ m ($a/l_u \sim 0.6$ and $\Delta z/l_u \sim 0.05$). At altitude $h = 360$ m we obtain $a \sim 624$ m, $\Delta z \sim 311$ m, and $l_u \sim 327$ m ($a/l_u \sim 1.9$ and $\Delta z/l_u \sim 0.95$). It is obvious that at an altitude of 360 m the spatial averaging is effective.
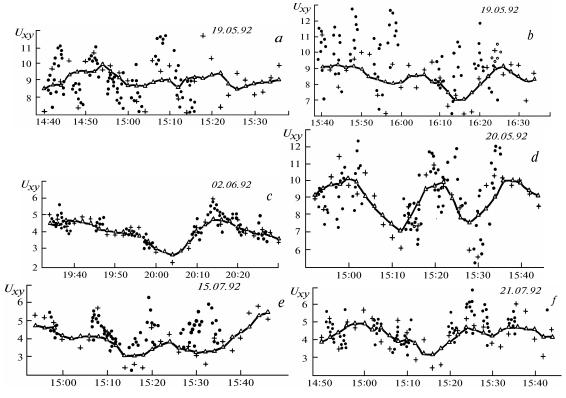

FIG. 6. *Lidar and cup-anemometer wind-velocity measurements.* $\varphi = 30°$: *neutral (a and d), stable (c), slightly unstable (e), and unstable (f) stratifications.* $\varphi = 60°$: *neutral stratification (b).*

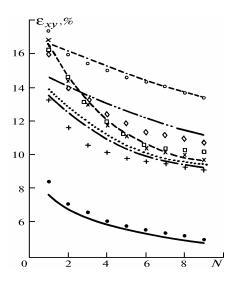FIG. 7. Errors in lidar mean wind velocity measurement. +, −.−.− are for the data of Fig. 6a; ×, − − − are for the data of Fig. 6b; •, −−−− are for the data of Fig. 6c; □, · · · are for the data of Fig. 6d; ◊, −··−··−·· are for the data of Fig. 6e; and, O, −−·−−· are for the data of Fig. 6f.
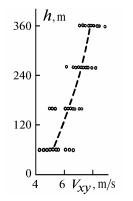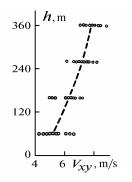

FIG. 8. Wind velocity profile.

FIG. 9. Lidar measurements error profile: ° experiment and − − − - theory.

CONCLUSION

Formula (9) derived in this paper allows us to estimate the error in the mean wind velocity measurement with the use of a scanning Doppler lidar taking into account the temporal and spatial averaging of the wind velocity fluctuations and turbulent state of the atmospheric boundary layer during the measurements. Theoretically calculated lidar measurement errors for different classes of thermal stratification have been compared with the errors in the experimental data. Satisfactory agreement of the theoretical results with the experimental data is indicative of the adequacy for the theoretical modes created in this paper to estimate the accuracy of lidar mean wind velocity measurements in the atmospheric boundary layer.

It has been shown that at the elevation angle $\varphi = 30°$, under conditions of the stable atmospheric stratification and at altitudes $h > 150–200$ m the mean wind velocity measurements become representative already for one revolution ($N = 1$) $\varepsilon_{xy} \lesssim 10\%$. In the case of neutral or slightly unstable stratification of the surface layer ($h = 60$ m), $N = 5$ provides for the error $\varepsilon_{xy} \lesssim 10–12\%$.

The authors would like to acknowledge M. Klier from the Institute of Optoelectronics and H. Kambezidis from the Athens Meteorological Institute for their assistance in carrying out the experiment as well as N. Kerkis from the Institute of Atmospheric Optics for his help in experimental data processing.

REFERENCES

1. Ch. Werner et al., *WIND. An Advanced Wind Infrared Doppler Lidar for Mesoscale Meteorological Studies.* Phase O/A-Study (1989).
2. F. Köpp, R.L. Schwiesow, and Ch. Werner, J. Climate Appl. Meteorol. **23**, 148 (1984).
3. Ch. Werner, Appl. Opt. **24**, No. 21, 3557–3564 (1985).
4. L. Kristensen and D.H. Lenshow, Amer. Meteorol. Soc. **4**, 128 (1987).
5. V.A. Banakh, F. Köpp, I.N. Smalikho, and Ch. Werner, Appl. Opt. (1994), to be published.
6. J.L. Lumley and H.A. Panofsky, *The Structure of Atmospheric Turbulence,* (Inter. publ., New York, 1964).
7. A.S. Monin and A.M. Jaglom, *Statistical Fluid Mechanics* (Nauka, Moscow, 1965), Vol. 1; (Nauka, Moscow, 1967), Vol. 2.
8. D.L. Laikhtman, *Physics of the Atmospheric Boundary Layer* (Gidrometeoizdat, Leningrad, 1961), 342 pp.
9. S.S. Zilitinkevich, *Dynamics of the Boundary Layer of the Atmosphere* (Gidrometeoizdat, Leningrad, 1970), 292 pp.
10. U. Hogstrom, Boundary-Layer Meteorology **42,** 55–78 (1988).
11. A.S. Monin, Izv. Akad. Nauk SSSR, Fiz. Atmos. Okeana **1**, No. 1, 45–54 (1965).
12. F.T.M. Nieuwstadt and H. Van Dop, *Atmospheric Turbulence and Air Pollution Modelling,* A Course held in the Haugue, 21–25 September, 1981.
13. B.G. Vager and E.D. Nadezhina, *Atmospheric Boundary Layer under Conditions of Horizontal Inhomogeneity* (Gidrometeoizdat, Leningrad, 1979), 136 pp.
14. A.K. Blackadar, J. Geophys. Res. **67**, No. 8, 3095–3102 (1962).
15. N.L. Byzova, B.N. Ivanov, and E.K. Garger, *Turbulence in the Boundary Layer of the Atmosphere* (Gidrometeoizdat, Leningrad, 1989), 263 pp.
16. L. Klristensen, T. Mikkelsen, and W. Aufm. Kampe, *Averaging for PBL Laser Doppler Measurements.*